Gravitational Wave Emission from Tight White Dwarf Binary Systems Formed Through Common Envelope Evolution

Juan Velasco

Instructor: Philip Arras

University of Virginia

Department of Astronomy

May 11, 2018

This thesis is submitted in partial completion of the

requirements of the BS Astronomy-Physics Major

Abstract

With the upcoming launch of the Laser Interferometer Space Antenna (LISA), the next natural candidates for merger observations are White Dwarf binaries. Current stellar mass candidates for gravitational wave sources suggest the existence of a mechanism which turns high period systems into low period ones. That is, if we hope to see mergers of such low-mass objects within the age of the Universe. In this paper we follow *Iben. Jr, Tutukov. (1986)*[1] to explore the different possible channels of mass transfer, Common Envelope Evolution and Stable mass transfer, as candidates for such mechanism. Using binary population synthesis code we evolve Helium White Dwarf binaries to attain a final mass and separation distribution. Our simulations found several configurations of initial masses and separation that lead to gravitational wave emission merger within the desired time frame. We also find a higher likelihood trend towards lower merger times in our results, ranging from 1.5×10^{-5} to 200 times the Age of the Universe. We determine stable mass transfer leads to the lowest merger times, but a mass gap around $0.25 M_{\odot}$. Unstable mass transfer leads to a lower mass discrepancy with *Iben. Jr, Tutukov. (1986)*[1].

Contents

1 Introduction

Gravitational wave observatories have an interest in predicting the merger rates of compact binaries throughout the whole universe. By comparing the expected and measured frequency of such merger events, physicists can place

tighter constrains on future theoretical models and discard current ones. For instance, calculating the population distribution of stellar remnants or finding an adequate equation of state which can describe the physics inside extreme density systems. With the advent of the Laser Interferometer Gravitational-Wave Observatory(LIGO), we have shared the luck of observing 6 mergers of binary black holes between 2015-2018. Another outstanding step was the recent discovery of a binary neutron star merger in 2018, the first of its kind. Then the question arises, what kind of mergers will we try to detect next? The natural progression would seem to suggest White Dwarf(WD) binaries are the answer. This intuition is further strengthened by the fact that 90% of stars are White Dwarfs and half of stars are found in binaries.[15].

We try to estimate if such mergers can even happen within the lifetime of Universe for low-mass systems. Taking from *Peters.(1964)*[6], setting the eccentricity $e = 0$ for circular orbit, the power emitted by 2 point sources $m1, m2$ with initial separation a emitting gravitational waves is

$$\frac{dE}{dt} = -\frac{32}{5}\frac{G^4 m_1^2 m_2^2 (m_1 + m_2)}{c^5 a^5} \tag{1}$$

We can derive an approximate timescale by simple arguments, since most of the time will actually be spent on the outward part of the orbit. Assuming this we use $E_{initial} = E_{orbital}$

$$\tau_{GW} \sim E_{initial}/\dot{E} = \frac{5}{64}\frac{c^5 a^5}{G^3 m_1^2 m_2^2 (m_1 + m_2)} \tag{2}$$

Plugging in characteristic value for WDs $m_1, m_2 = 1M_\odot$ and $\tau_{GW} = t_H$ the age of the Universe, we solve for the initial separation $a = 2.3R_\odot$. At first this sounds impossible since binaries can't be that close. Unless there was a mechanism that could reduce the orbital separations in binary systems. In *Pacynzski.(1976)*[3] such a mechanism was introduced through Common Envelope tidal interactions. The torques and drag generated by the envelope would lead to inspiral of the binary components, thereby effectively starting with a new system at lower initial separation. The intent was to try to explain phenomena such as Cataclysmic variables, where there is a WD orbiting with a Main Sequence companion, at very short separation. Such systems should not be possible, since the WD had to originally undergo an expansion phase when exiting the Main Sequence. Hence, the natural explanation is that they were originally further apart, and moved in closer through some process. Over time the Common Envelope Evolution(CEE) became a more refined model, for example *Webbink.(1983)*[2] introducing the energy formalism

$$\Delta E_{orbital} = -\Delta E_{Binding} \tag{3}$$

This equation, even in its most primitive form encapsules the physics of how the trade in energy can lead orbital shrinkage and period reduction. Sample systems such as the binary WD pair L870-2 are believed to have experienced two phases of CEE. This is the case considering the low period of $1day, 6hours$ and separation $\sim 5.8R_\odot$.[8] Using the upcoming LISA mission,

we will we able to detect several more systems like these. In the meanwhile, we can keep relying on binary population synthesis, models were several sample masses and separations are generated using distribution functions. By generating huge ensembles, these models turn statistical descriptions of initial conditions into predictions. For instance, predicting the gravitational wave merger rates and times, which is what was attempted at in this paper. Last clarification, everything is by default assumed to be in units of $M_{\odot}, R_{\odot}$ and t_H for the rest of the paper, in case of a function or plot is given without units.

2 White Dwarfs

White Dwarfs are the end states of low mass stars, like our Sun. Once low mass stars reach the end of the Main Sequence, as the Hydrogen burning ceases and gravitational collapse ensues, the core contracts. For stars below about $8M_{\odot}$, they will not be massive enough to become a neutron star or black hole. If the mass is not high enough, the star will not reach temperature high enough to burn heavier elements, such as He, C or O. If ignition does not occur, the remnant from gravitational collapse will be a core sustained by degeneracy pressure. This pressure arises from the exclusion principle, which prohibits identical Fermions from occupying the same quantum states simultaneously. Hence, electrons inside a WD or neutrons inside a neutron star can only be packed so closely together. White Dwarfs have similar masses

to neutron stars, around $1M_{\odot}$. However, they are much smaller, with an average size around the Earth radius, compared to $10km$ for a neutron star. We model non-relativistic White Dwarfs as a polytropes with index $n = 3/2$, so the pressure is given by

$$P = K\rho^{(n+1)/n} = K\rho^{5/3} \tag{4}$$

If we include relativistic considerations of the cosmic speed limit c, the resulting equation of state is softened. The new equation of state, for a fully degenerate relativistic core is a polytrope of index $n = 3$

$$P = K\rho^{4/3} \tag{5}$$

That is as the velocity of the electrons inside the WD approach c, the momentum flux is constrained by the upper bound of the speed of light. We use the mass radius relationship for WDs

$$R_{WD}(M) = R_{\odot}\left(\frac{M}{M_{\odot}}\right)^{-1/3} \tag{6}$$

which tells us higher mass WDs are actually smaller. Hence higher mass leads to tighter packing, bringing the electrons together. By the Heisenberg Inequalities, we get a bigger spread in the velocity of the electrons until eventually relativity kicks in. This leads to the Chandraskhar mass $M_{Ch} = 1.44M_{\odot}$ as the upper bound for the WD masses. Any WD beyond this point collapses into a neutron star, which is not the topic of this paper. Hence in our

simulations we pick masses lower than $8M_{\odot}$ to ensure we only generate WDs that will not surpass M_{Ch} upon leaving the Main Sequence. However, we are interested in the results of gravitational wave emission mergers, which will produce remnants with a fraction of the combined mass of the components. Through this channel of formation, we can explain the formation of low-mass single He WDs. Since most low-mass HeWDs show up only in binary systems, this is actually an exotic sighting to study.

3 Gravitational Waves

Gravitational waves are very hard to detect in general, even coming from massive Black hole binaries. Back at Earth, the received amplitude of waves from these mergers generate effects 3 orders of magnitude lower than the size of a proton. However, LIGO's 4km interferometer arms have managed to tame the low amplitude problem. Now the limiting factors on Earth are the vibrational modes of the Earth, which are impossible to decouple from Earth-grounded systems. However, LISA will use 3 laser interferometers orbiting the sun in a triangular configuration, lagging behind the Earth as depicted in Fig(1).

Hence LISA will not be limited by Earth's tectonic noise. Instead it must face with it's own kind of noise, acceleration noise. This noise is generated by magnetic and gravitational field fluctuations that perturb the masses in the detectors, which are to remain stationary with respect to each other.

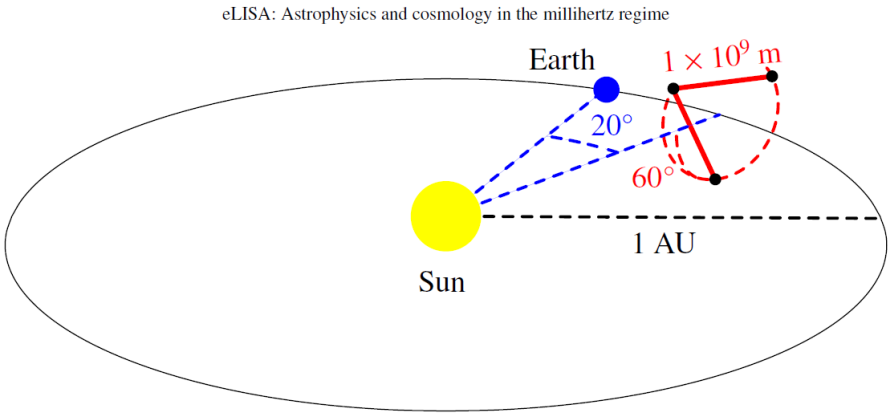

Figure 1: Scheme of the trajectory of LISA[4]

As shown in Fig(2), LISA will have to deal with acceleration limits at low frequencies. However, Fig(3) shows how LIGO isn't even close to those ranges of Frequencies. LISA will be the first gravitational observatory to probe frequencies lower than $10^{-2}Hz$, thereby expanding the horizons of what we can detect. Current predictions are that binary WD sources will dominate the landscape of LISA's observations, being flooded with the vast population of such systems.[4] Some binaries which have already been detected through other means can be further studied through observations of gravitational waves. For those many which are not verification binaries, we can have a first glimpse into these faint systems which are not detectable through regular means. These systems also posses extremely low periods, on orders of minutes, so they are heavily believed to have undergone at least one phase of Common Envelope Evolution. With such low periods, gravitational wave emission leads to merger of such systems on short time scales, so they are

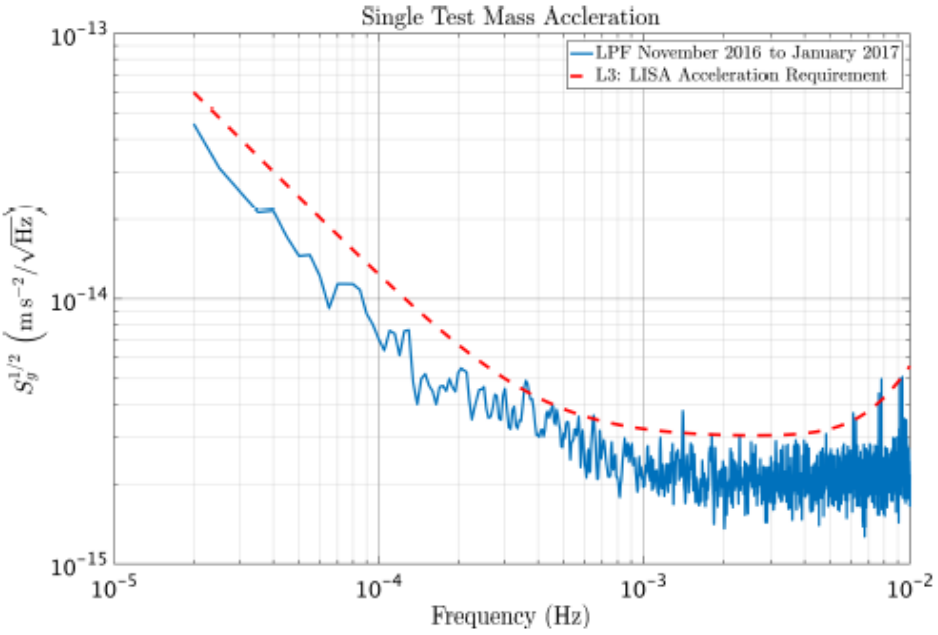

Figure 2: Acceleration noise limits on the strain for low frequencies[5]

short lived.

Motivated by this, we try to find the exact lifetime τ_{GW} of tight binary systems decaying through gravitational wave emission. Again using Eqn(1) we now equate it to the time derivative of the initial orbital energy.

$$\frac{dE}{dt} = \frac{d}{dt}\left(-G\frac{m_1 m_2}{a}\right) = G\frac{m_1 m_2}{a^2}\dot{a} \tag{7}$$

Where if we solve for $\dot{a}$ we get the differential equation

$$\dot{a} = \frac{-64}{5}\frac{G^3 m_1 m_2 (m_1 + m_2)}{c^5 a^3} \tag{8}$$

which gives the corresponding solution

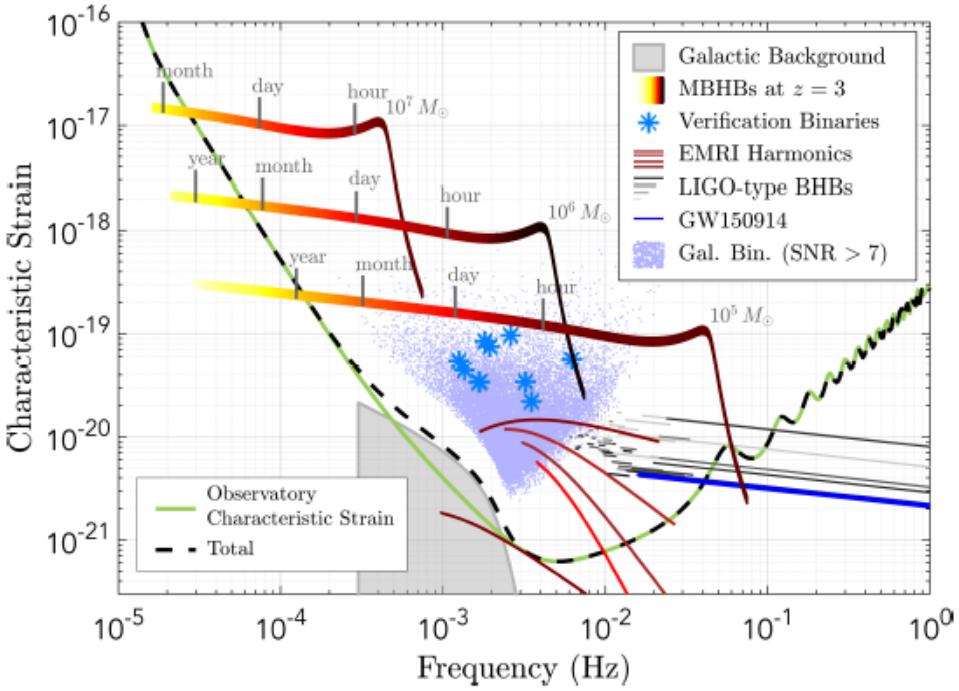

Figure 3: Comparison of targets visible by LISA and LIGO, with noise constrains for LISA[5]

$$a(t) = \left(a(0)^4 - t \quad \frac{256}{5} \frac{G^3 m_1 m_2 (m_1 + m_2)}{c^5 a^3} \right)^{1/4} \tag{9}$$

Now solving the condition for merger $a(\tau_{GW}) = 0$ we find

$$\tau_{GW} = \frac{5}{256} \frac{a^4 c^5}{G^3 m_1 m_2 (m_1 + m_2)} \tag{10}$$

which yields answer only 4 times smaller than our original derivation using basic algebra. However, the exact function is necessary to get a better estimate of the actual merger time, which we would've overestimated had we just used the approximation. A similar derivation using the rate of loss of angular momentum would've yielded the exact same answer, since the rates are the same up to constants.

4 Mass Transfer Mechanisms

Binary stars, are not always exciting systems. If the orbital separation of the system is too wide, they will basically evolve independently. Hence, we want to focus our attention on low separation systems, which can interact with each other and lead to interesting results such as Cataclysmic Variable stars or Novae. The leading models to explain these kinds of objects posit these are formed through mass exchange between a close binary pair. Working with binary systems is easier by choosing coordinate systems centered on the centered of mass, so the coordinates are not moving over time, but everything

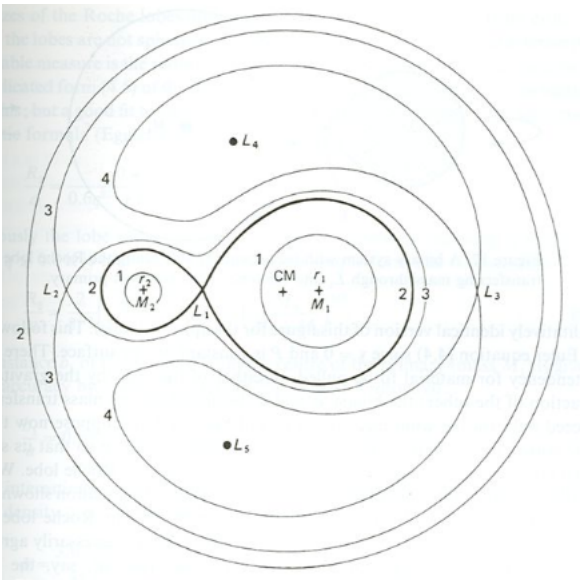

Figure 4: Depiction of gravitational potential surfaces with the Lagrange points[8]

moves around it.If we want to know how the binary evolves, we need to consider the gravitational interactions between the components. We look at surfaces of equal gravitational potential, since we want to determine the regions where each star's gravitational influence dominates. Fig(4) shows the surfaces of interest, and also the Lagrange points, where the potentials of both stars match.

For close enough regions to the star, these surfaces are spherical, so we can find the radius of a sphere bounding the volume where a star's potential dominates. We define this approximate radius for each star to be it's Roche Lobe. We define the first Roche function approximation used in *Iben.Jr,Tutukov.(1986)*[1]

$$R_{Roche} = a \quad .52 \left(\frac{M_{donor}}{M_{donor} + M_{accretor}} \right)^{0.44} \tag{11}$$

where M_{donor} is the star losing mass, $M_{accretor}$ is the companion and q is the mass ratio

$$q = \frac{M_{donor}}{M_{accretor}} \tag{12}$$

The second expression for the Roche Lobe we use is given by *Eggleton.(1982)*[10]

$$R_{Roche} = a\ r_L \quad , \quad r_L = \frac{0.49q^{2/3}}{0.6q^{2/3} + ln(1 + q^{1/3})} \tag{13}$$

which is accurate to 1% and r_L is the dimensionless radius called the Roche ratio. The $L1$ point is where the Roche Lobe's of both stars meet, and hence mass transfer can occur through this point and become bound to the companion. Mass transfer can begin if one the stars swells and grows beyond it's Roche Lobe, so that mass becomes unbound. We consider the scenario of leaving the Main Sequence after Hydrogen burning reaching the threshold of 10% burning. A Helium core will be left over, which grows as given by *Iben.Jr,Livio.(1993)*[8]

$$R_s = R_{\odot} 10^{3.5} \left(\frac{M_{He}}{M_{\odot}} \right)^4 \tag{14}$$

Where R_s is the stellar radius of the donor during the Red Giant Branch

Phase. There are 2 possible scenarios of mass transfer, unstable and stable. If the donor loses mass, it will lead to its radius and Roche Lobe decrease. If the Roche lobe decreases faster than the radius of the donor, then the star will keep losing mass faster, in positive feedback loop. In this runaway case, it can lead to Common Envelope Evolution. If the radius, decreases faster then the mass transfer will stop, but will resume periodically for short periods. This will lead to a stable exchange of mass which occurs over longer timescales.

4.1 Common Envelope Evolution

For unstable Roche Lobe overflow, mass will start to be ejected from the the donor at alarming rates. The mass will go through the L1 point and build up on the companion. If the mass transfer is fast enough, ie: it happens on dynamical time scales, then the mass will not be able to be accreted effectively by the companion. Hence, during this evolution phase we regard the secondary as remaining constant in mass. This will lead to a build up of a convective envelope around both stars, as the mass accretes past the Roche Lobe of the secondary. This is because the time it takes to return to Hydrostatic Equilibrium is many orders lower than the Thermal timescale. We require the envelope to be convective, so as more mass is lost, mass bubbles from below will convect upward to replenish the envelope, due to the convective instability. Then energy and angular momentum, will be deposited into the envelope, which will cause it to be ejected. In this paper

we only consider orbital energy of the binary which is used to eject the envelope and reduces the orbital separation, making the binary more bound. We add an extra term α to Eqn(3) to account for the efficiency at transferring orbital into unbinding the envelope[8]

$$\alpha = \frac{\Delta E_{Binding}}{\Delta E_{Orbital}} \tag{15}$$

Physical considerations, such as conservation of energy require alpha to be lower than 1, when considering no other energy sources. That is because any ejecta from the envelope will exit with some no-zero kinetic energy. We take the expression for the orbital energy to be:

$$\Delta E_{orbital} = -G\frac{M_{core}M_{accretor}}{2a_F} + G\frac{M_{donor}M_{accretor}}{2a_i} \tag{16}$$

but we also have approximations like that of *Iben.Jr,Tutukov.(1986)*[1]

$$\Delta E_{orbital} \sim -G\frac{M_{core}M_{accretor}}{2a_F} \tag{17}$$

neglecting the initial orbital term under the assumption that the final separation a_F is much smaller than the initial one a_i. For the gravitational binding we have:

$$E_{bind} = -G\frac{M_{env}M_{donor}}{\lambda a_i r_L} \tag{18}$$

which tries to estimate the envelope M_{env} as if it were spherical, with the

radius being the Roche Radius $R_L = a_i r_L$ and being bounded to the itself and the core. The λ factor is an attempt at correcting for the assumption of using a simple spherical approximation. This is dependent on every star, and contains information about the thermal structure of the primary. We take it to be constant for simplicity. Some other possible approximations, as used by *Iben.Jr,Tutukov.(1986)*[1] take the assumption that the core mass resulting from CEE is very low

$$E_{bind} \sim -G\frac{M_{donor}^2}{\lambda a_i r_L} \tag{19}$$

Another possibility is modeling the envelope having a radius a_i(without the r_L factor) and being binded to both the primary and secondary star, as done in *Iben.Jr,Livio.(1993)*[8]

$$E_{bind} = -G\frac{M_{env}(M_{donor} + M_{accretor})}{\lambda a_i} \tag{20}$$

Throughout the paper we make the substitution $\beta = \alpha\lambda/2$ since both constants show up together and their product is normally taken to be 2 so $\beta = 1$. Combining the gravitational binding expressions, with the orbital enregy expressions and Eq(15) we get three different functions for the final orbital separation after a phase of CEE

$$a_F = a_i \quad \frac{M_{core}M_{accretor}}{2\beta M_{donor}^2} \tag{21}$$

$$a_F = a_i \quad \frac{M_{core}}{M_{donor} + \beta M_{env} M_{donor}/r_L M_{accretor}} \tag{22}$$

$$a_F = a_i \quad \frac{M_{core}}{M_{donor} + \beta M_{env}(M_{donor} + M_{accretor})/M_{accretor}} \tag{23}$$

4.2 Stable Mass Transfer

Consider the case where the orbital separation gets larger by mass transfer, hence a will grow and so will R_L. Hence, even if the primary initially achieves Roche Lobe overflow, it will become halted. This model for conservative mass transfer relies on two assumptions, conservation of mass and angular momentum in our isolated system

$$M = M_1 + M_2 = const \quad , \quad L = \mu\ell = const \tag{24}$$

Where μ is the reduced mass of the binary system and ℓ is the specific angular momentum, ie: the angular momentum per mass

$$\mu = \frac{M_1 M_2}{M} \quad , \quad \ell = \sqrt{GMa} \tag{25}$$

Putting these constrains together and solving for a gives a proportionality to the masses, which can be turned into a ratio to give

$$a_F = a_i \left(\frac{M_{1i} M_{2i}}{M_{1F} M_{2F}} \right)^2 \tag{26}$$

Hence we have a new function for the final separation after an event of mass transfer. It is important to note, as opposed to having the primary lose mass and the secondary being constant, in this case the secondary actually accretes mass. Since the time scales are on the order of the thermal one, there is enough time for the material to fall in get acrreted by the secondary. Hence we will see an increase in the secondary mass equivalent to the mass loss of the primary.

5 Probability Distributions

In order to generate a population of stars, we required a mass distribution function and a binary separation distribution function. The mass distribution used was the Saltpeter Initial Mass function[9]

$$\mathbb{P}_M(M) = \frac{1}{N_1}\left(\frac{M}{M_\odot}\right)^{-2.35} \quad , \quad 0.8 < \frac{M}{M_\odot} < 30 \tag{27}$$

which gives an estimate of the birthrate of a star of a given mass M in our galaxy. This formula is valid in the range stated above, but we chose our bounds of integration to be those used in *Iben.Jr,Tutukov.(1986)*[1]

$$\int_{1M_\odot}^{2.3M_\odot} \mathbb{P}_M dM = 1 \tag{28}$$

and hence we get our normalization constant N_1 from this condition. Then we can simply integrate this probability distribution analytically, to yield a Cumulative Probability Function(CDF):

$$CDF_M(M) = \int_{1M_\odot}^{M} \mathbb{P}_M dM = \frac{1}{N_1}\left(\left(\frac{M}{M_\odot}\right)^{-2.35} - 1\right) \tag{29}$$

By definition of the CDF, it satisfies the conditions:

$$0 = CDF_M(1_\odot) \leq CDF_M(M) \leq CDF_M(2.3M_\odot) = 1 \tag{30}$$

So we can use this function to sample our choice of masses, by generating a random number in the interval $[0, 1]$ and solving for M. While not fully accurate, we assume the probabilities for two masses M_1, M_2 in a binary are independent. Hence, we get the simple product

$$\mathbb{P}_{2M}(M_1, M_2) = \frac{1}{N_2}\left(\frac{M_1 M_2}{M_\odot}\right)^{-2.35} = \mathbb{P}_M(M_1)\mathbb{P}_M(M_2) \tag{31}$$

So we can use the formulas stated above to calculate the binary mass distribution using the single mass distribution. In a similar manner, the orbital separation a distribution function, taken from *Popova.(1982)*[14]

$$\mathbb{P}_a(a) = \frac{1}{N_3}\left(\frac{a}{R_\odot}\right)^{-1} \tag{32}$$

where we impose the normalization condition

$$\int_{2R_\odot}^{292R_\odot} \mathbb{P}_a da = 1 \tag{33}$$

which when integrated yields the CDF

$$CDF_a(a) = \frac{1}{N_3} \ln\left(\frac{a}{2R_\odot}\right) \tag{34}$$

satisfying analogues conditions to Eqn(30). Again, assuming independence of probabilities, we decompose the total probability function as a product

$$\mathbb{P}_{a,2M}(a, M_1, M_2) = \mathbb{P}_a(a)\mathbb{P}_{2M}(M_1, M_2) \tag{35}$$

So we can generate all our quantities a, M_1 and M_2 with no constrains other than belonging to the ranges delimited by our integration. In the next section we will elaborate on the criteria for selection of bounds.

6 Simulations

Using the probability distributions mentioned in the previous section, we produced a binary population synthesis. Calling 3 instances of a random number generator *random.random* in Python and combining with the CDFs yielded a triplet (a_i, M_{1i}, M_{2i}). We begin by checking for nonphysical condi-

tions, such as immediate merger if the initial separation is smaller than the sum of the radii of the stars. Since our initial stars are assumed to be Main Sequence Stars, we use the relation for the radius[14]

$$R_{MS}(M) = R_{\odot}\left(\frac{M}{M_{\odot}}\right)^{0.8} \quad , \quad \frac{M}{M_{\odot}} \geq 1 \tag{36}$$

The next consideration is the initial masses cannot be too low, or else they won't reach the end of the Main Sequence in the span of the age of the Universe, taken to be the Hubble time $t_H = 13.7 \times 10^9 yr$. Using an approximation for the MS lifetime

$$t_{MS}(M) = t_{\odot}\left(\frac{M}{M_{\odot}}\right)^{-2.5} \tag{37}$$

we derive a lower bound for the mass $M_{min} = .88M_{\odot} \sim 1M_{\odot}$ consistent with our earlier definition of CDF_M. The upper-bound choice for the mass is derived from considerations of Eqn(14), which is only valid in the regime of masses smaller than $M_{max} = 2.3M_{\odot}$. For the separation minimum we defined it to be $a_{min} = 2R_{MS}(M_{min})$, since we want to avoid unnecessary mergers on the onset of our simulation. Note, we do not choose what seems more logical option $2R_{MS}(M_{max})$ which would prevent all nonphysical beginnings, since we still want to probe the behavior of systems with very low initial separation. The maximum value was derived from the Roche Lobe Eqn(11) combined with the core mass-stellar radius relation in Eqn(14), when $q = \frac{M_{max}}{M_{min}} = 2.3$ yielding the lowest upper-bound $a_{max} = 292R_{\odot}$. Fig(5) shows an attempt

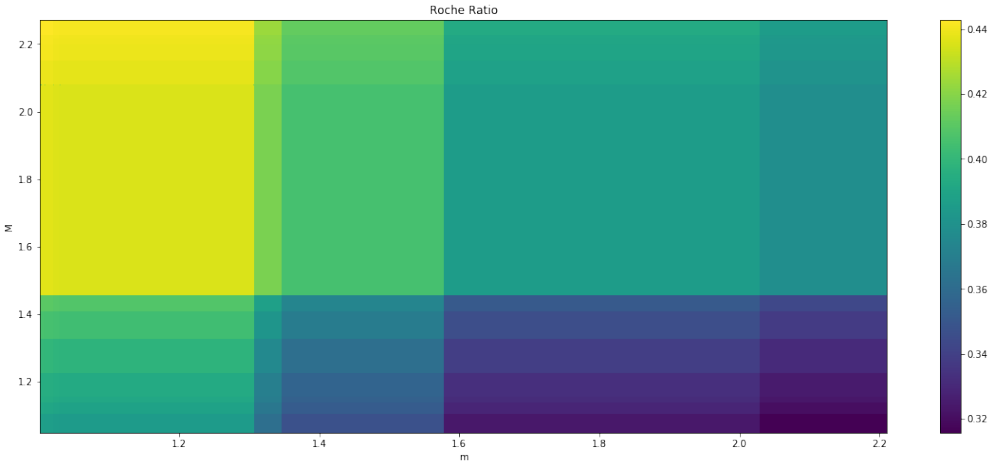

Figure 5: Minimization of Roche ratio within our mass constrains, where M is the primary more massive star and m is the secondary, in units of $M_{\odot}$

.

at finding the minima for the Roche ratio r_L function by testing masses in our desired range. We categorize any failure to comply these requirements with $status = 0$. Taking these limits into account, we only produce masses and separations which will minimize the number of non-physical situations, while still preserving a vast of range of combinations to explore.

Once we have a triplet which satisfies the criteria, we can undergo the first phase of mass transfer between the stars. We begin by setting the primary $M_{donor} = max(M_{1i}, M_{2i})$, since the more massive star will have shorter lifespan on the Main sequence and become a red giant. That leaves $M_{accretor} = min(M_{1i}, M_{2i})$ for the secondary. In this part of the process is where we branch off, trying two different paths of evolution. As done in *Iben.Jr,Tutukov.(1986)*[1], we consider the two possibilities of the first

phase of mass transfer being stable or unstable. Regardless of our choice of evolutionary track, we calculate the final masses and separation assuming the primary star fills it's Roche Lobe. We do this by equating the Roche Radius with the stellar radius, and calculating the core mass derived from that. Our simulations also explored the difference in results by using the two different expressions for the Roche Radius in Eqn(11) and Eqn(13). First, if the final mass of the primary is above the desired limit $M_{core} = .45M_{\odot}$, we terminate that simulation and bin that in the results corresponding to $status = 1$. What this physically corresponds to, is the failure of the primary to actually fill it's Roche Lobe. While this star might still achieve Roche Lobe overflow on it's next stage on the AGB, we are only concerned in studying degenerate He WDs for this paper. Hence, we disregard the possibilities of C,O WDs undergoing mass transfer by filling their Roche Lobe after exhaustion of He burning. Second, if the final separation is lower than the sum of the radii of the stars, we consider this a merger, binned as $status = 2$ and the simulation terminates. In this stage we use the WD mass-radius relation Eqn(6) for the degenerate core that remains from the primary.

If all is clear, we go on to carry out a second phase of mass transfer, which we always take to be unstable and lead to CEE. We now reverse the roles, taking the donor to be the secondary star, which may have changed mass depending on our choice of stable or unstable mass transfer in the first phase. Setting the star radius equal to it's Roche Radius, we split again into 3 different branches, depending on our equation for Common Envelope.

Repeating the same checks we did after the first mass transfer scenario, we return a $status = 3$ if the final mass of the secondary M_{2f} exceeds $.45 M_{\odot}$. Using the WD radius formula for both remnants now, we determine if the sum of the radii is smaller than the final separation, in which case we return $status = 4$.

Assuming we pass all this checks, we are finally left with a triplet (a_f, M_{1f}, M_{2f}) corresponding to a physical system, which has undergone changes in orbital separation and mass of it's components. We now apply Eqn(10) to determine the time τ_{GW} it would take for this binary to decay through Gravitational wave emission and eventually merge. If the time required for inspiral surpasses the age of the Universe, we return $status = 5$. If the time scale is shorter, we have found a good candidate and return $status = 6$. Throughout this process, we store the separation and mass of each stellar component at each stage, initial, middle and final. We also return the *status* label to sort the output by their outcome, and for example bundle all the initial configurations which yield binaries which don't merge through mass transfer events and go on to emit Gravitational waves. We then repeat all these steps 10^5 different times, to sample our binary population distribution adequately. We note that while the reference paper does this with 10^7 data points, carrying out some comparisons showed the same results converging around 10^5 points. Hence we kept the lower the number of points, choosing to minimize running time, which scaled from seconds to minutes to fractions of hours.

	1^{st} Mass Transfer	2^{nd} Mass Transfer
No Roche Lobe Overflow	1	3
Merger	2	4

Nonphysical setup	0
$\tau_{GW} > t_H$	5
$\tau_{GW} < t_H$	6

Table 1: Summary of status values corresponding to different outcomes

7 Results

We begin by recapping our status classification system in Table(1), which will be used in the plots for the rest of this paper.

We proceed to examine the comparison of effects of choosing among the 3 different CEE functions in Eqn(21).Eqn(22) and Eqn(23). The first thing to notice in both Fig(6) and Fig(7) the approximation used by *Iben.Jr,Tutukov.(1986)*[1] yields the highest number of candidates for gravitational wave emission which will merge within the Hubble time for both channels of mass transfer. On the other hand, the formula used by most papers, such as *Webbink.(1983)*[2] the second highest number of gravitational wave-emitting pairs. The double core bound envelope function is outperformed by the other 2 functions for the stable mass transfer case. However, it is the most effective at generating binaries which will have merger times longer than the age of the universe. The biggest difference between the 2 channels of mass transfer is the relative quantity of WDs that go on to merge after 1 phase or 2 phases of Roche Lobe overflow. Given all this we adopt our default CEE function to be the approximation function, since it generates the highest number of candidates,

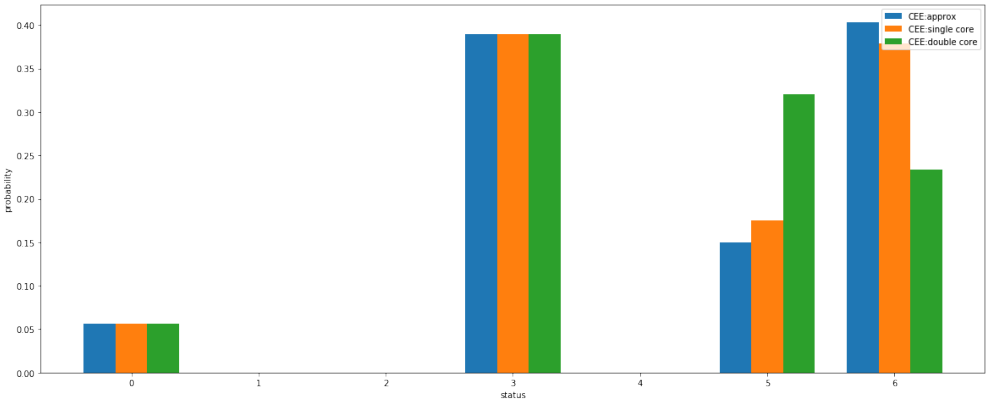

Figure 6: Difference in outcomes using different CEE functions for stable followed by unstable mass transfer

.

without giving results way off from the full formula.

We then look at the comparison in results for the two expressions for the Roche Radius. In Fig(8) we can see there exist a visible difference in the probability distribution of outcomes when we do stable and unstable mass transfer. However, the results are unchanged for the case of two phases of unstable mass transfer in Fig(9). This is surprising, since it tells us that the outcome of the binary relies more heavily on the Roche ratio for long time scale processes. This should be intuitive, since in CEE the transfer of mass is so fast that the system has no time to respond to the change in Roche ratio. However, for the slower mass transfer case, a the discrepancy piles up over time. For the rest of the paper we take the Roche function to be that of *Iben.Jr,Tutukov.(1986)*[1].

Another more important factor to consider is the β constant, which has

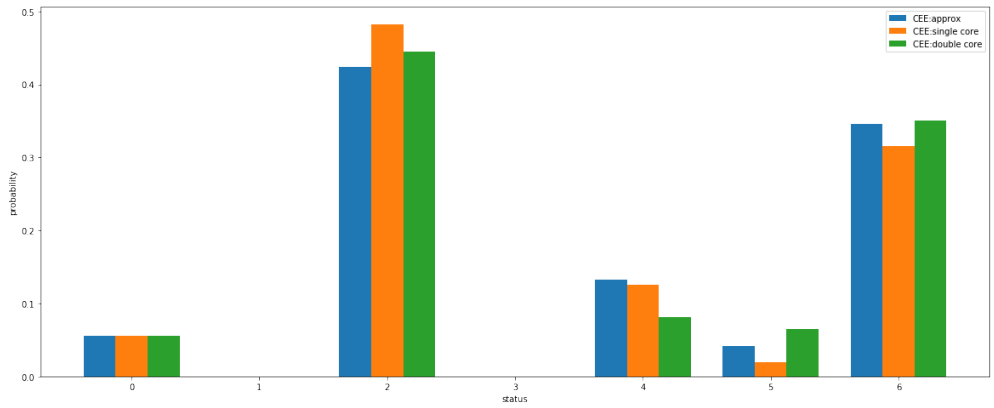

Figure 7: Difference in outcomes using different CEE functions for double unstable mass transfer

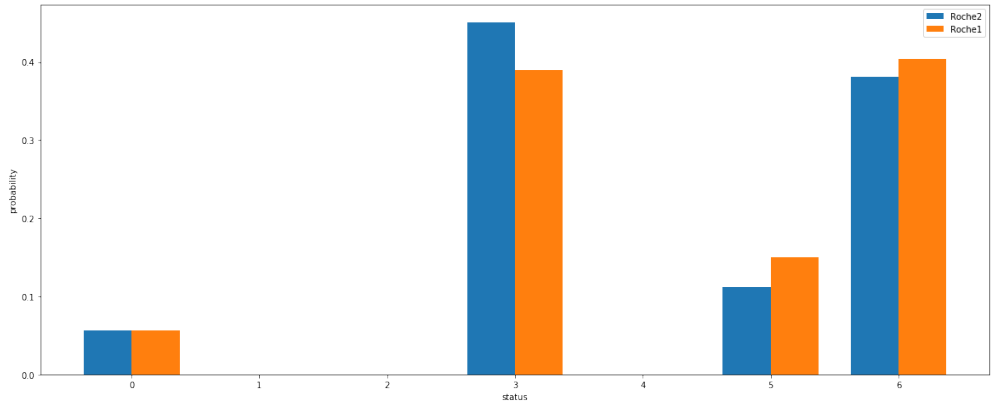

Figure 8: Difference in outcomes using different definitions of the Roche Lobe for stable followed by unstable mass transfer

.

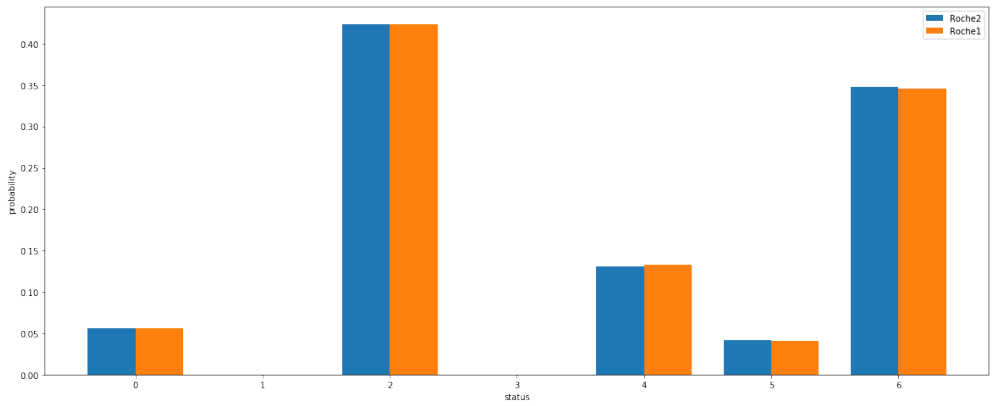

Figure 9: Difference in outcomes using different definitions of the Roche Lobe for double unstable mass transfer

a great effect in determining the transfer of energy between components in the system. In Fig(10) we can see that this factor basically determines the frequency of outcomes that are not mergers through mass transfer. For high values of β, for example $\beta = 2$ we get an increase in good binaries by 2 orders of magnitude from the lowest values. In Fig(11) we notice the same effect that β has opposite effects at different phases of mass transfer. For the first mass transfer, higher β leads to lower merger rates, but does the opposite during the second mass transfer phase. For the remainder of the paper we take the value $\beta = 1$ by default.

In Fig(12), after fixing the CEE functions, Roche function and β we can finally compare the 2 channels of mass transfer one on one. The first thing to notice, which is a common factor across all other figures for double CEE evolution, is that we only get mergers or gravitational wave emission as results. That is the Helium cores never surpass the critical value of $0.45 M_{\odot}$.

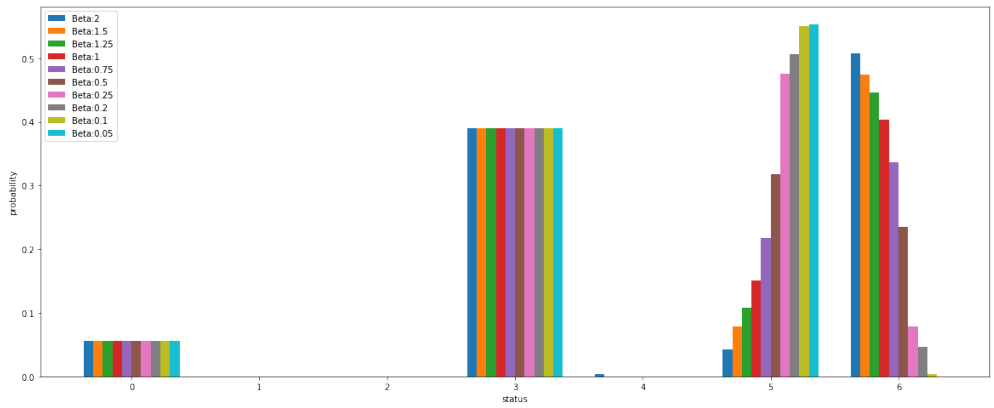

Figure 10: Difference in outcomes using different β values for stable followed by unstable mass transfer

.

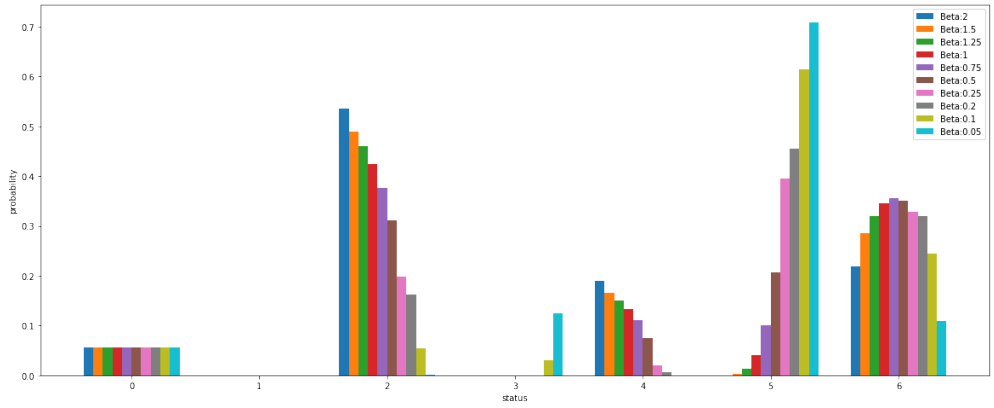

Figure 11: Difference in outcomes using different β values for double unstable mass transfer

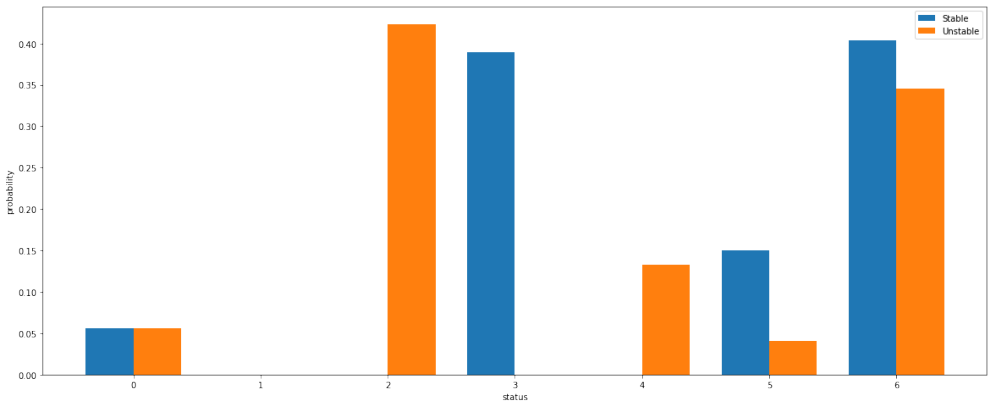

Figure 12: Difference in outcomes using different β values for double unstable mass transfer

Since the core mass is proportional to the radius of the star, which we set to be the Roche radius, we have a direct proportionality on the orbital separation. Since CEE can only decrease the separation, the secondary will have a much lower Roche radius and hence the core growth will stop very early. However, if we include the first stable mass transfer phase, the orbital separation gets increased, and hence gives the primary more time to grow it's Helium core before hitting the Roche radius. Moreover this is why see we see an empty $status = 2$ for stable mass transfer, since a increases so the stars will not merge. That gap occurs for the unstable channel at $status = 1$ and $status = 3$, since the second core can only grow smaller than the first one, so if the first one fails to overflow, so will the second one. We conclude that the stable channel followed by unstable mass transfer is the best mechanism for generating binaries which will be close enough to each other to merge.

The images comparing the final distributions after stable and unstable

mass transfer range from Fig(13) to Fig(19) for successful creation of Gravitational wave binary WDs(GWBWDs). We see the unstable transfer generates many more lower separations, showing its effectiveness at bringing stellar bodies close together. The stable channel on the other hand generates a more spread out distribution of final separations. The next figure shows that stable mass transfer can be more effective at stripping off mass from the primary, since the peak of the distribution is much lower than that of CEE. As expected CEE generates lower final masses for the secondary, since the core has little time to accrete due to low separation distances. An interesting observation is that the stellar companions that started as the lower mass star are now reaching the $0.45M_{\odot}$ threshold to the right of Fig(15), thanks to the increase in a and mass acrreted. In Fig(16) we can appreciate the relation between initial minimum mass and initial maximum mass changes over time. For the stable mass transfer, only those cases where the secondary core ends up being more massive than the core of the primary do we get GWBWDs. However this never happens for unstable mass transfer, the primary always ends up being more massive the secondary, since a only decreases. Interestingly the candidates for GWBWDs end up having masses very different from each other, most commonly having the more massive one being double the lower mass one.

Fig(17) is a very important one, since it shows the final abundance of masses of binaries after double CEE phase or a stable followed by unstable phase. We compare this plot to Fig(18), which contains *Iben.Jr,Tutukov.(1986)*[1]

results of their simulations for dN/dM, basically the abundance per mass in binaries, which is up to scaling the final probability distribution. Our work in this paper is focused on a special case of their plot, their Helium Dwarfs curve. However, our plots clearly don't match as expected. First of all, we would expect a continuous population of WDs between $0.2M_{\odot}$ and $0.45M_{\odot}$, with a peak around $0.25M_{\odot}$. Our results show roughly two peaks, one around $0.15M_{\odot}$ and the other one around $0.35M_{\odot}$. The most contrasting difference is the clear gap in masses around $0.25M_{\odot}$ in the stable formation channel. The unstable channel suffers from a less pronounced lack of masses around $0.25M_{\odot}$. Another sanity check is looking at the distribution of values for the merging time τ_{GW} in Fig(19). We notice they seem to follow a preference for lower merging times. The most important takeaway is that lower merger times are more common, since CEE combined with CEE is more likely to form lower orbital separations.

Only for those configurations that lead to GWBWDs we compare the effects of a single phase of mass transfer, to see what it does to the initial distributions of orbital separation a, initial maximum mass M and initial minimum mass in the binary m. We begin by examining the plots for the effects of CEE, ranging from Fig(20) to Fig(23). We first remark the effectiveness of CEE at reducing the orbital separation and also the fact that only long initial separations lead to GWBWDs. We can clearly see the higher mass M undergoes heavy mass loss, given little time to build the core it will preserve after ejecting the envelope. The mass of the the secondary on the

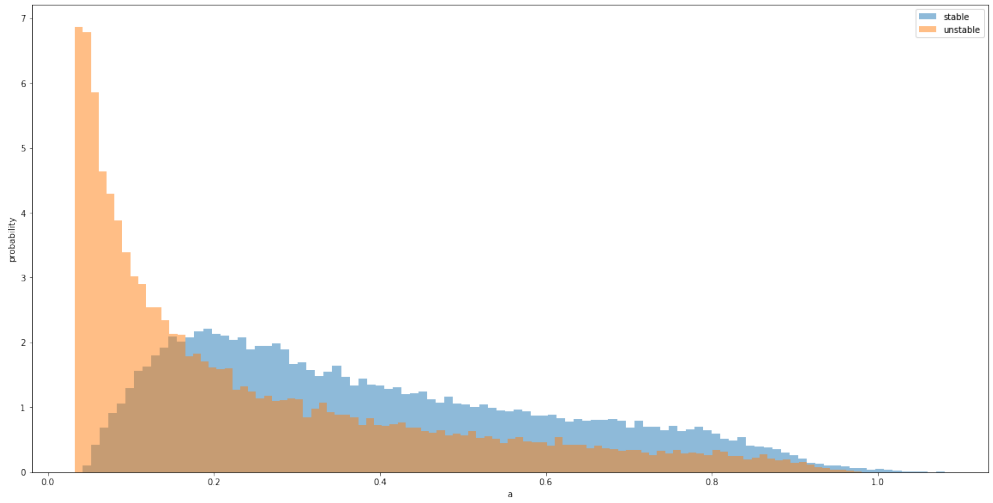

Figure 13: Comparing the final distributions after each types of mass transfer on initial orbital separation a distribution

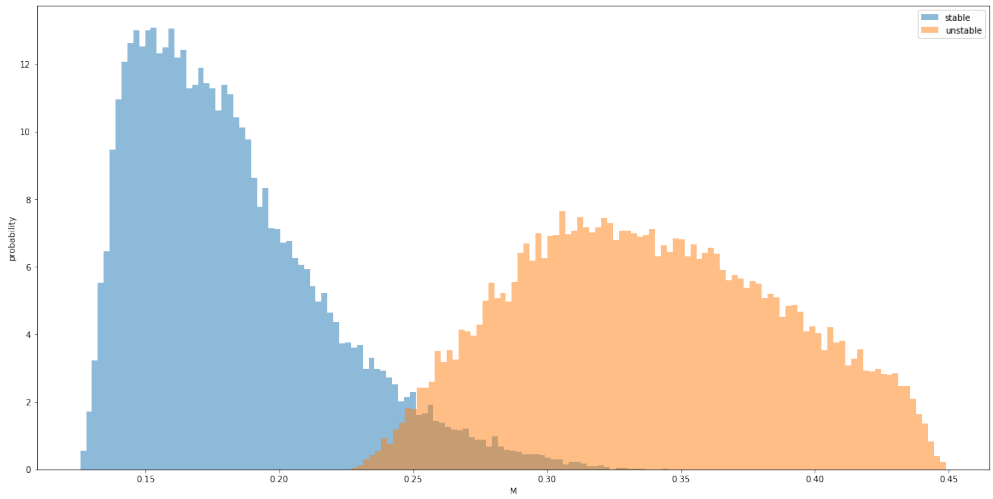

Figure 14: Comparing the final distributions after each type of mass transfer on maximum initial mass M distribution

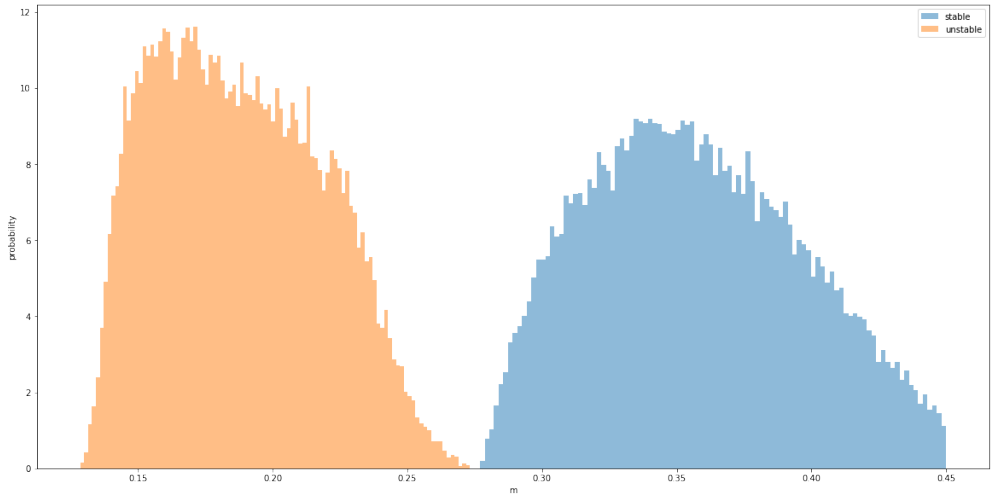

Figure 15: Comparing the final distributions after each type of mass transfer on minimum initial mass m distribution

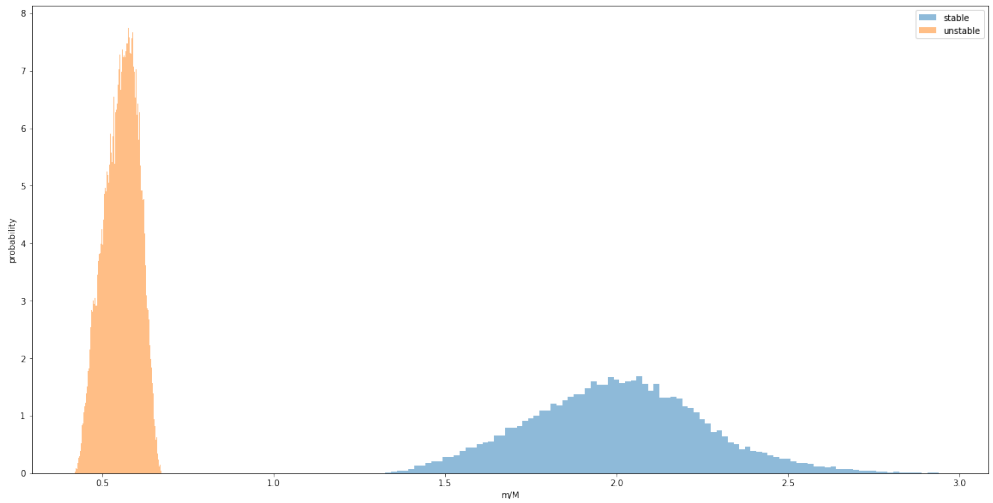

Figure 16: Comparing the final distributions after each type of mass transfer on m/M initial minimum mass over initial maximum mass distribution

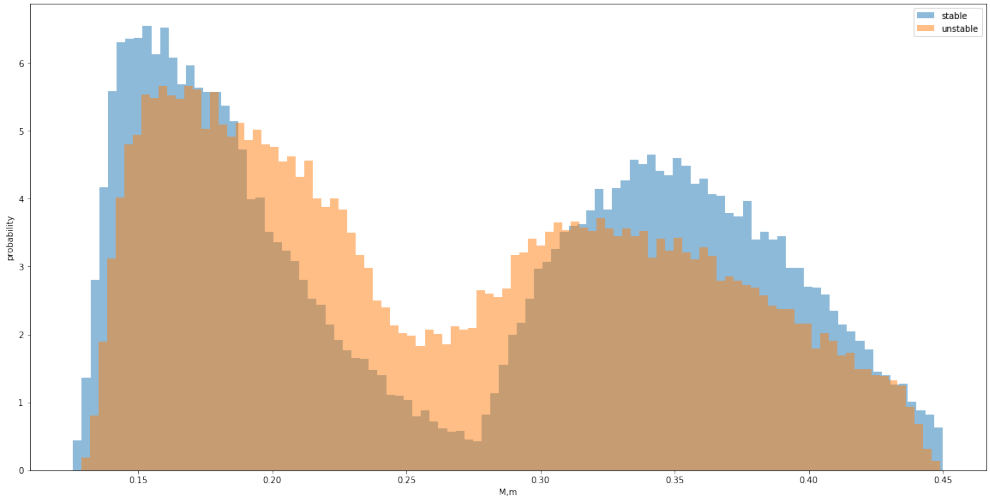

Figure 17: Comparing the final distributions after each type of mass transfer on combined mass distribution

other hand is unaffected, since there is not enough time for the companion to accrete the mass landing on it. This is shown by the perfect overlap of the two distributions.

The images relating to the effects of stable mass transfer range from Fig(24) to Fig(27). As expected, the effect of stable mass transfer is to increase the initial orbital separation to an order of magnitude larger than the initial one. The primary mass M not only decreases, but the secondary has the ability to feed off that mass lost. The net result is having much higher masses and orbital separations to begin CEE with, thereby leading to larger remnants for the secondary.

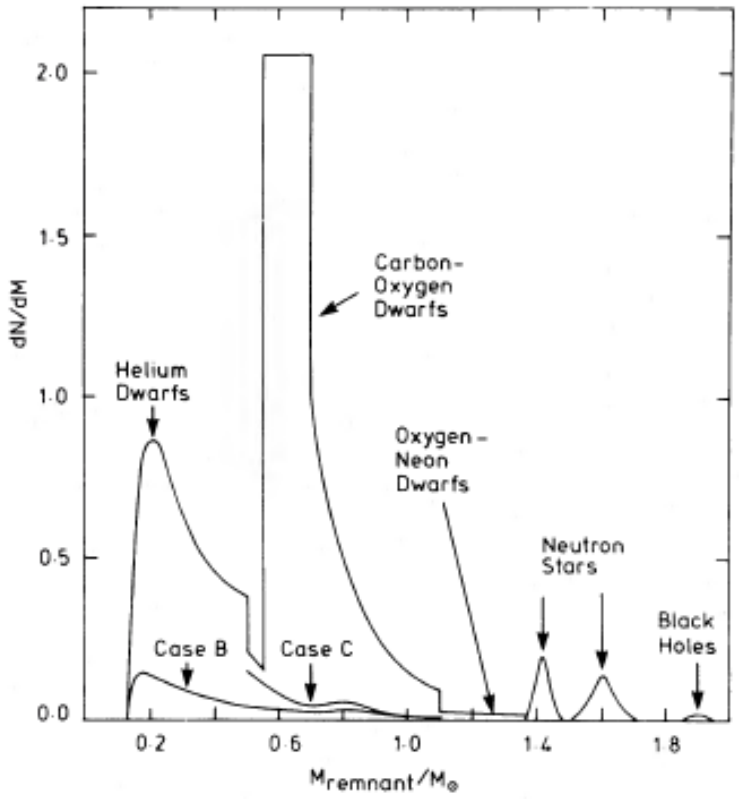

Figure 18: Distribution of masses from *Iben.Jr,Tutukov.(1986)*[1]

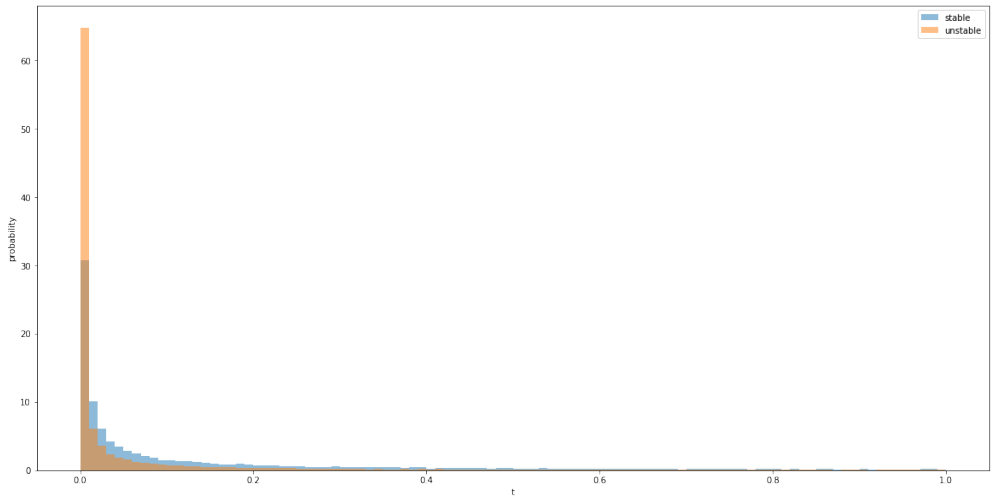

Figure 19: Comparing τ_{GW} the gravitational wave emission merger time after each type of mass transfer in units of Hubble time t_H

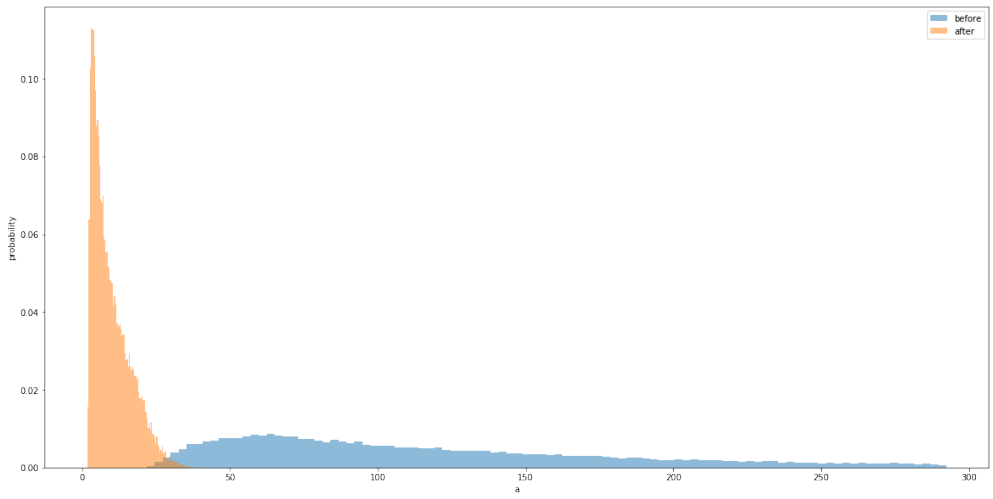

Figure 20: Effects of CEE on initial orbital separation a distribution

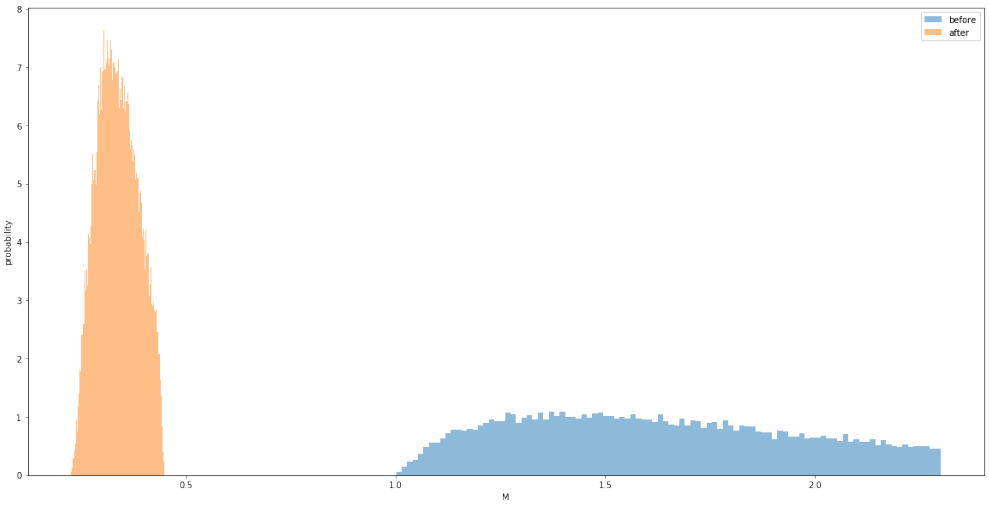

Figure 21: Effects of CEE on maximum initial mass M distribution

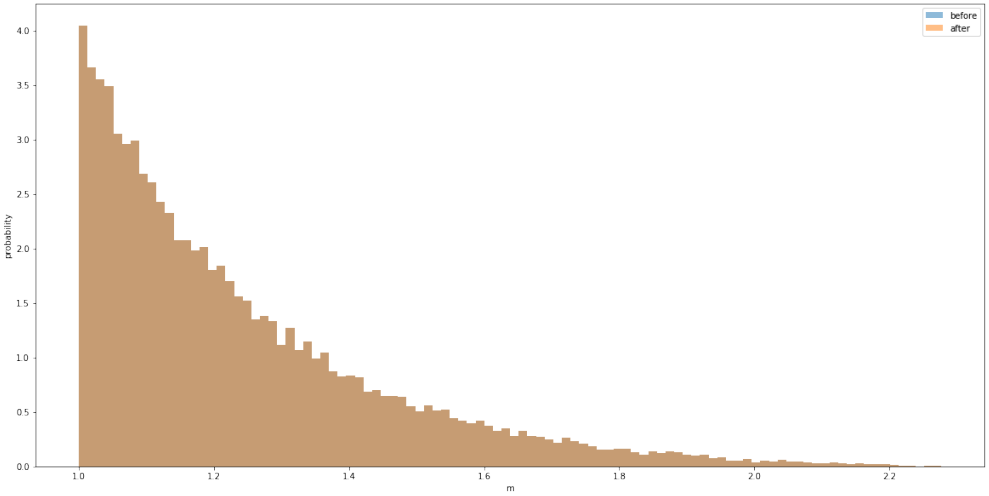

Figure 22: Effects of CEE on minimum initial mass m distribution

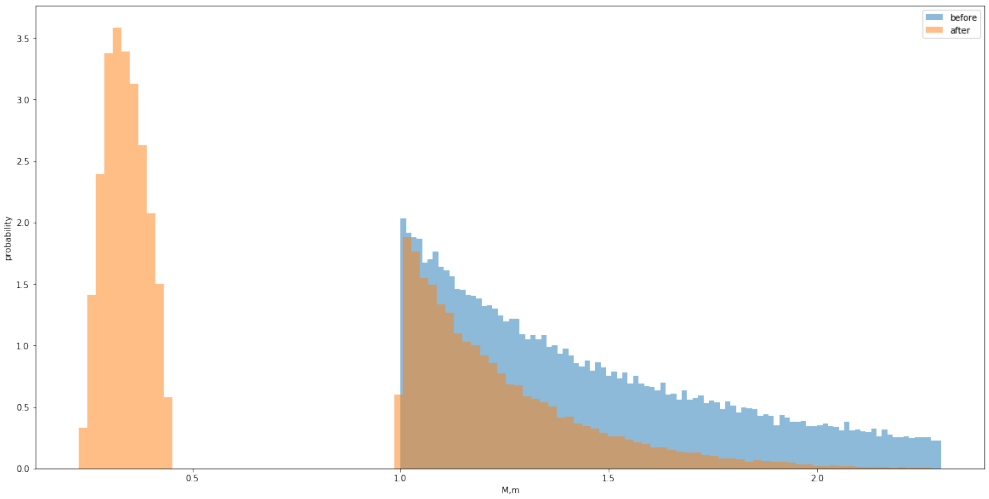

Figure 23: Effects of CEE on combined mass distributions

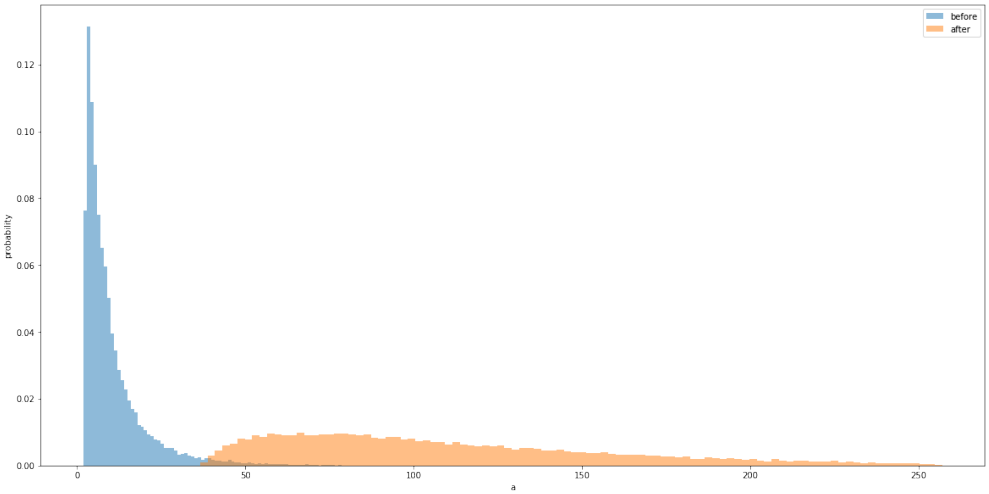

Figure 24: Effects of stable mass transfer on initial orbital separation a distribution

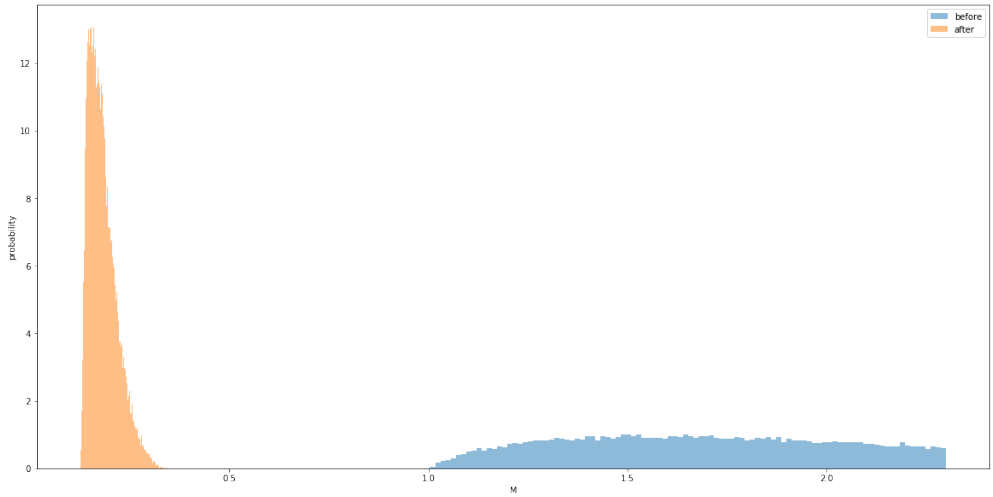

Figure 25: Effects of stable mass transfer on maximum initial mass M distribution

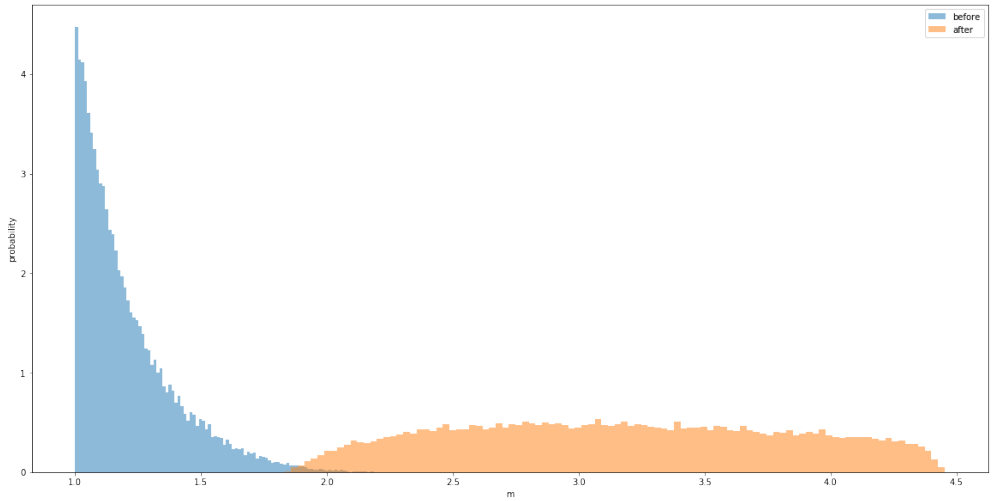

Figure 26: Effects of stable mass transfer on minimum initial mass m distribution

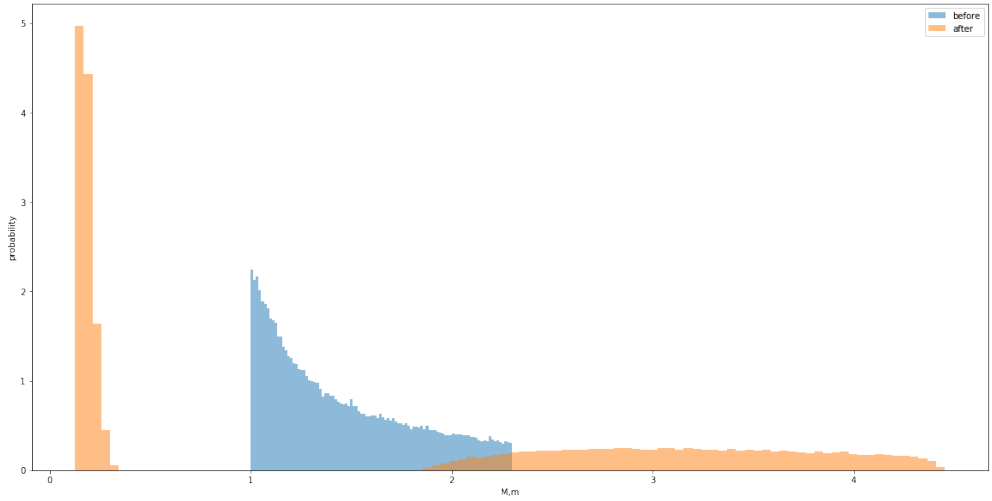

Figure 27: Effects of stable mass transfer on combined mass distributions

8 Discussion

It is hard to ignore the discrepancy in the final mass distribution plots with that of *Iben.Jr,Tutukov.(1986)*[1]. The lack of masses in the middle of the distribution could be a coding error or could say something about the physics of CEE we forgot to account for. Now we clarify some of the assumptions which were brushed aside in the illustrations of the steps carried out. In this simple model we disregard any thermal structure of the star, evolutionary effects or interactions with other sources of energy, like radiation or magnetic fields. Hence, we set β to be a constant among all out stars, of which the importance of considering in more detail is highlighted in *Dewi,Tauris*(2000)[11], *Tauris,Dewi*(2001)[12]. Another big thing is the change in composition due to accretion of mass through the stable chan-

nel of mass transfer, since the secondary will be getting a mix a of it's original material and a big share of the primary's. We assume there always happen 2 phases of mass transfer, which is not always the case for real life systems. We take q, the mass ratio, to be a constant during the mass transfer event which might not be very accurate for stable mass transfer which lasts over longer periods of time. Another simplification is assuming that core growth immediately stops when the star grows to match it's Roche Lobe. Basically, doing this evolution seems to require too many simplifications, which might be too computing-intensive to account for all of them. However, this toy seems to be good enough at predicting GWBWDs. We get the lowest merger time for stable mass transfer to be $1.5 \times 10^{-5} t_H$ which is much lower than the lower merger time for unstable mass transfer $.998 t_H$. From this and Fig(19) we conclude that the stable mass channel is the best candidate mechanism for generating GWBWDs.This does not exclude future considerations of alternative formation channels. There always exists the possibility of my code being wrong and in order to fix that would probably require rewriting a few parts from scratch. Future work might include trying to make the plots with expectations match or at least determine the source of the discrepancies, which still alludes us.

Bibliography

[1] Iben, I. & Tutukov, A. V. 1986, , 311, 753.

[2] Webbink, R. F. 1984, , 277, 355. compare

[3] Paczynski, B. 1976, Structure and Evolution of Close Binary Systems, 75.

[4] Amaro-Seoane, P., Aoudia, S., Babak, S., et al. 2013, GW Notes, 6, 4.

[5] Amaro-Seoane, P., Audley, H., Babak, S., et al. 2017, ArXiv e-prints , arXiv:1702.00786.

[6] Peters, P. C. 1964, Physical Review, 136, 1224.

[7] Zhang, X.-F., Liu, J.-Z., Jeffery, C. S., et al. 2018, Research in Astronomy and Astrophysics, 18, 9.

[8] Iben, I. & Livio, M. 1993, Publications of the Astronomical Society of the Pacific, 105, 1373.

[9] Salpeter, E. E. 1955, , 121, 161.

[10] Eggleton, P. P. 1983, , 268, 368.

[11] Dewi, J. D. M. & Tauris, T. M. 2000, , 360, 1043.

[12] Dewi, J. D. M. & Tauris, T. M. 2001, Evolution of Binary and Multiple Star Systems, 255.

[13] Ivanova, N., Justham, S., Chen, X., et al. 2013, Astronomy and Astrophysics Review, 21, 59.

[14] Popova, E. I., Tutukov, A. V. & Yungelson, L. R. 1982, , 88, 55.
Stellar Multiplicity. Annu. Rev. Astron. Astrophys. 2013

[15] Duchêne, G. & Kraus, A. 2013, Annual Review of Astronomy and Astrophysics, 51, 269.